Self-Powered, Room-Temperature Electronic Nose Based on Triboelectrification and Heterogeneous Catalytic Reaction

*Ji-hyun Kim, Jinsung Chun, Jin Woong Kim, Won Jun Choi, and Jeong Min Baik**

Herein, a self-powered electronic nose strategy with highly selective gas detection is described. The electronic nose is a two-dimensional microarray based on the triboelectrification between ZnO nanowires and the dielectric layers, and the heterogeneous catalytic reaction occurring on the nanowires and on the NiO nanoparticles. These electronic noses show the ability to distinguish between four volatile organic compound (VOC) gases (methanol, ethanol, acetone, and toluene) with a detection limit of 0.1% at room temperature using no external power source.

1. Introduction

Chemical and biological sensor technologies have received much attention in the last decade and have undergone great developments because of their profound impact on personal safety, detection of toxic pollutants, and recently, on the proliferation of the internet of things (IOTs).[1–3] So far, most works have focused on the development of sensor technologies with high sensitivity and selectivity. Many groups have successfully demonstrated such sensors by fabricating a variety of multi-component sensor arrays, known as electronic noses.[4–6] With recent advances in wearable electronics, the electronic nose is expected to provide us with reliable and sustainable healthcare services through big data processing. This approach will speed-up the commercialization success of electronic-nose technologies. However, the larger the number of sensors in the array the bigger the power supply needed. Many innovative ways to reduce the power consumption in sensors have already been suggested.[7,8] However, the realization of self-powered sensors that are capable of detecting several gases without the need of external power sources is critical to increase the performance of electronic noses.

Very recently, a triboelectric nanogenerator (TENG), which harvests energy by physically contacting two materials with different triboelectric polarities from ambient mechanical energy sources, has been suggested as a new harvesting technology. TENGs have been proven to generate quite large output powers and many self-powered sensors have been successfully demonstrated using TENGs.[9,10] TENG systems have been effective in enhancing the adaptability, portability, and durability of these sensors.[11–14] However, the attempts so far have been focused purely on the change in electrical output performance when the TENGs were exposed to the gases. The presence of the gases usually reduces the surface triboelectric charges, thereby, decreasing the electrical output signals of the TENGs.[9,10,15] This is a fundamental property of the gas detection mechanism by triboelectrification . However, these approaches have not shown sufficient selectivity, therefore, the sensor technologies to increase the selectivity are still needed.

In this paper, for the first time, we describe a strategy for creating a self-powered electronic nose with high gas selectivity that is operable at room temperature. In most electronic noses, various factors, such as different materials, temperature gradients, sensor designs are employed for the multi-component sensor arrays.[16–18] Here, we propose a principally different approach, whereby the arrays are based on the triboelectrification effect caused by the physical contact between the semiconducting nanowires (ZnO) and the dielectric films, as key materials in the fabrication of self-powered electronic noses. The ZnO is partially functionalized with nickel oxide (NiO) nanoparticles (NPs) to enhance the heterogeneous catalytic processes. Our sensor shows a range of molecular specificity based on gas molecular recognition through a lock-and-key-type model. Continuing the catalysis theme, polyimide and PTFE were attached as dielectric materials to the top electrode (Al), in a direction which was orthogonal to that of the NiO NPs on the ZnO. The two dielectric materials were chosen according to the difference in their triboelectric polarities and surface tensions (i.e., the surface tension of polyimide is about 2.8 times larger than that of PTFE). Thus, the electrical output will be significantly modified by the different dielectric layers.

The electronic nose that we designed was used to detect four volatile organic compounds (VOCs), such as methanol, ethanol, acetone, and toluene. These compounds are known to be easily evaporated from adhesives, paint, synthetic building materials, etc., which are all regarded as health risk problems.[19,20] The efficient monitoring of such VOCs is essential in environmental and public safety control because of the potential health hazards when exposed to these gases. So far, there have been many reports on the VOCs sensing, however,

J.-h. Kim, J. Chun, J. W. Kim, Prof. J. M. Baik
Department of Materials Science Engineering
KIST-UNIST-Ulsan Center for Convergent Materials
Ulsan National Institute of Science
and Technology (UNIST)
Ulsan 689–798, Republic of Korea
E-mail: jbaik@unist.ac.kr
W. J. Choi
Electronic Materials Research Center
Korea Institute of Science and Technology (KIST)
Hwarangno 14-gil 5, Seongbuk-gu
Seoul 136–791, Republic of Korea

DOI: 10.1002/adfm.201503419

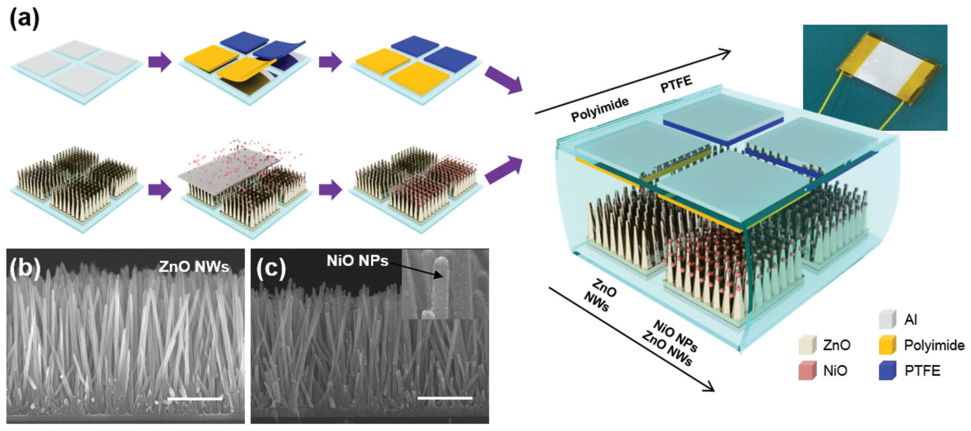

Figure 1. a) Schematic illustration of the fabrication process of a self-powered electronic nose and an optical image of the as-fabricated device. SEM images of b) the ZnO nanowires and c) the NiO NPs-decorated ZnO nanowires grown on the SiO_2/Si. The NiO nanoparticles are also shown in the inset of (c). The post-annealing process at 600 °C induces an aggregation of the Ni films into well-separated NiO nanoparticles covering the nanowires uniformly. The scale bar in (b) and (c) is 500 nm.

the selectivity is still considered as one of the most difficult issues because of their similar compositions and molecular structures.[21]

2. Results and Discussion

Figure 1a shows the schematic diagram of the sensor array and detailed information about the fabrication process is described in the Experimental Section. In short, ZnO nanowires of 80 nm in diameter and 2 μm in length were grown on a ZnO seed layer that was deposited on a SiO_2/Si substrate. A 5-nm thick (mass thickness) Ni film was deposited using electron-beam evaporation at a base pressure of 3.0×10^{-6} Torr through a shadow mask to functionalize the surface of the nanowires. The metal films aggregated into NiO nanoparticles of 20 nm in size after annealing at 600 °C, as shown in Figure 1. Polyimide and PTFE were used as dielectric materials and placed on an Al film deposited by electron-beam evaporation. When the fabrication process was completed, each 2×2 array functioned as one sensor element, consisting of different dielectric materials and NiO nanoparticle decorated nanowires.

First, we measured the sensing properties of the nanowires at an applied voltage of 1 V, an Al film without dielectric layer was used as the top electrode and was located on top of the nanowire arrays, after which copper wires were then adhered on both electrodes with silver paste. **Figures 2**a and 2b show current–voltage characteristics as a function of time for pristine and NiO NPs-decorated ZnO nanowires, respectively. One of the four VOCs gases was periodically introduced to the surface of the sensor arrays in an air-conditioned atmosphere and then the gas flow was shut off. Representative values of the sensitivity and the response time of the sensor towards the gases are given in Figure 2c. The sensitivity could be defined as $S = (I_g - I_a)/I_a$, in which I_g and I_a are, respectively, the steady-state current values measured at room temperature with and without the gas introduced in the air-conditioned atmosphere. For pristine ZnO nanowires, the acetone gas flow increased the current for less than 7 min, returning to its initial value reversibly within 13 min when the gas was shut off, while there was

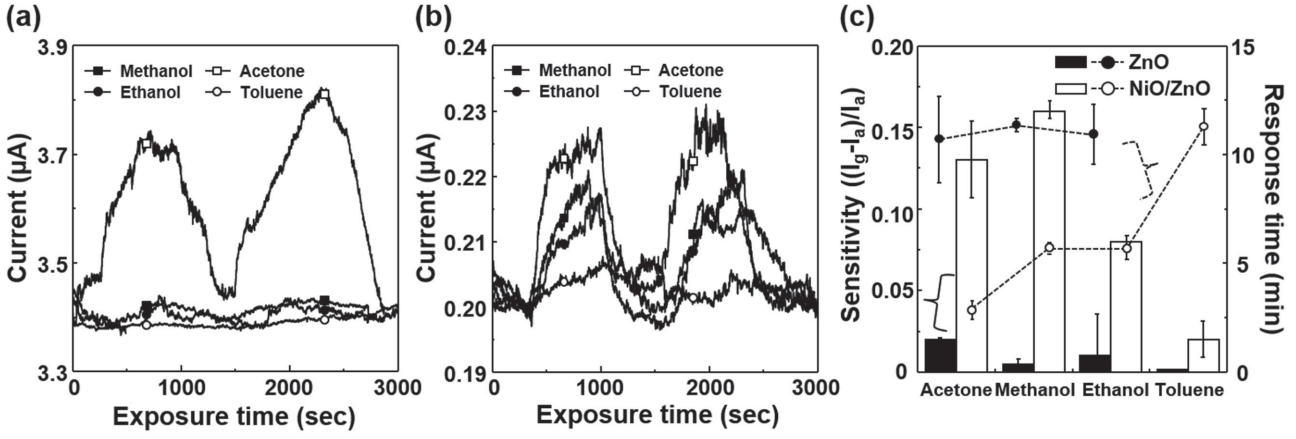

Figure 2. a,b) Representative sets of current measured as a function of time at an applied voltage of 1 V. The change in current of the devices comprising a) pristine and b) NiO NPs-decorated ZnO nanowire sensor toward methanol, ethanol, acetone, and toluene measured at room temperature. c) Representative values of the sensitivities and response times of the sensor for the four gases.

no significant change in the current for the other gases. VOC gases are known to be reactive towards many of the surface sites (such as chemisorbed surface oxygens) present on the surface of ZnO, where they are oxidized to species such as CO_2 and H_2O.[20,22] The reaction can at the same time reduce the oxide, leading to an increase of the current from molecule-to-nanowire electron donation. However, we found no significant increase in the current for other gases than acetone, although there was a little increase in the current for the methanol and ethanol gases. This may be ascribed to the large dissociation energy of such molecules on ZnO nanowires at room temperature, compared with the dissociation energy (393 kJ mol^{-1}) of acetone.[23]

When decorated with NiO, the sensitivities towards the gases increased. As reported previously, the large increase in sensitivity toward VOC gases can be ascribed to the charge-depletion layer formed at the interface of the p–n junction.[24] When a p–n junction is formed, the depletion region increases in width, thereby increasing the resistance of the oxides, as shown in Figure 2b. The NiO particles can also act as a catalyst to promote the oxidation reaction by not only increasing the amount of absorbed oxygen, but also decreasing the activation energy of catalytic oxidation.[24,25] Thus, in the presence of VOC gases the electron concentration in ZnO increased whereas the concentration of holes in NiO decreased, thus giving rise to a lower resistance of the ZnO nanowires and thereby increasing the sensitivity. The decrease in the response time may be due to the rapid diffusion of the gas molecules and the promotion of the surface reaction by the NiO particles.[26,27]

Then, we inserted the dielectric layers (PTFE and polyimide) between the Al electrode and the nanowires. The two electrodes were connected through an insulating polymer with double-sided adhesive with a thickness of 0.03 mm, maintaining a gap, as shown in Figure 1a. **Figure 3**a,b presents the output voltages, obtained from each of the sensor elements exposed to ethanol gas under a cycled compressive force of 50 N at an applied frequency of 4 Hz. In the absence of ethanol gas, the output voltage in the TENG consisting of ZnO nanowires and a PTFE film was about 2.4 V, however, the output voltage decreased to about 0.3 V when the PTFE was replaced by the polyimide. This may be ascribed to the relatively less negative triboelectric polarity of the PI film in the triboelectric series, compared to that of the PTFE film.

Ethanol gas flow across the ZnO nanowires caused the output voltage to decrease steadily from 2.4 V to 1.5 V after about 4 min of ethanol exposure at room temperature. When the gas was terminated, the output voltage returned reversibly to its initial value, however, the recovery was slow (>10 min). When the PTFE was replaced by the polyimide and exposed to the gas, the output voltage decreased by about 0.1 V. The sensitivity could be defined as $S = (V_g - V_a)/V_a$ in this device, in which V_g and V_a are the output voltages measured in the

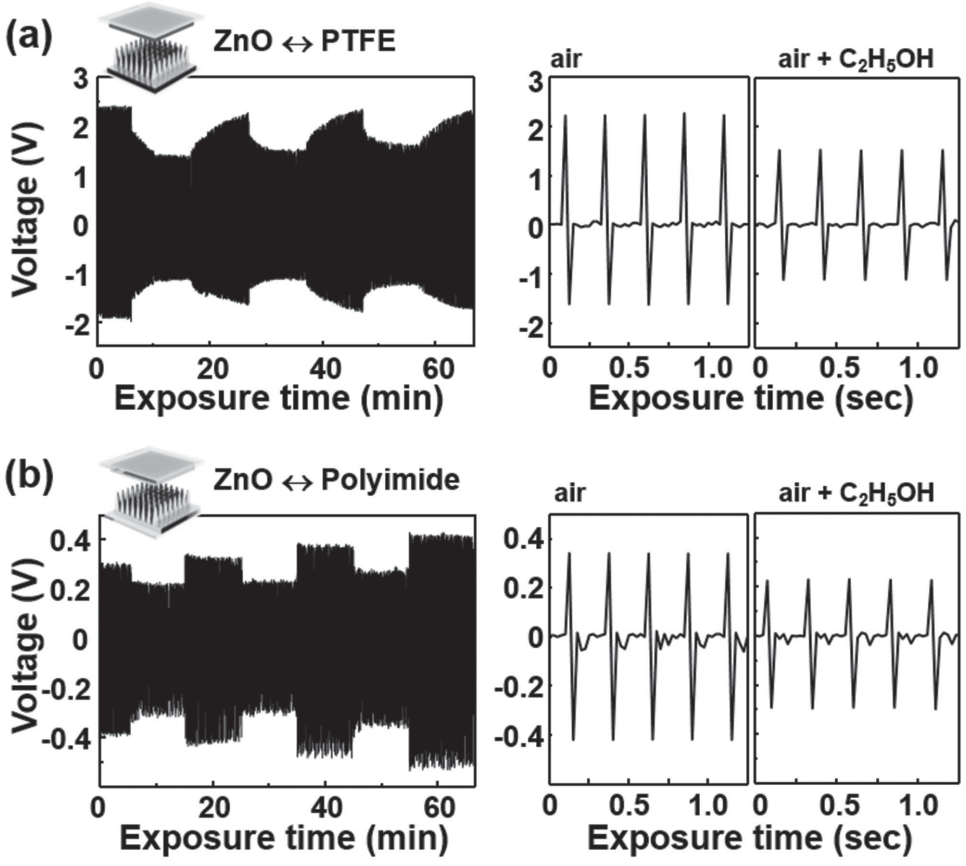

Figure 3. The output performance of the sensor elements comprising a) ZnO-PFTE and b) ZnO-PI under a cycled compressive force of 50 N at an applied frequency of 4 Hz. The enlarged output voltages of each sensor element are also shown here.

presence of VOCs gases and air, respectively. It can be seen that there is no significant change in the sensitivity between both TENGs although the sensitivity decreased a little from –0.38 to –0.33 using the PI film. However, it can clearly be seen that the output voltage decreased and recovered much faster when using PI instead of PTFE (<10 s). Representative values of the sensitivities and response times of the sensor towards the gases are given in Figure S1 in the Supporting Information. The output voltages as a function of applied compressive force from 10 N to 90 N and ambient relative humidity from 20% to 80% were also measured and the sensitivities are plotted in Figures S2 and S3 (Supporting Information). The sensitivity and response time are comparable with those of previously reported metal oxide nanowires.[23,28,29]

In general, the power generation in TENGs under a cycled compressive force is usually explained by the coupling of the triboelectric effect and electrostatic induction.[30,31] The periodic contact between the two materials brings about electron transfer (e.g., from the ZnO to the dielectric layer), resulting in positive charges on the ZnO nanowires and negative ones on the dielectric layer. This produces an electric potential difference when they are separated, driving an electron flow through the external circuit. The electrical output is determined by the density of the triboelectric charges generated on both surfaces.[32,33] The charge density is usually reduced when the surfaces are exposed to VOC gases because the molecular species on both surfaces reduce the triboelectrically charged area.[9,15,34,35] The different behavior in the response time in Figure 3a,b may be caused by the different levels of surface wettability of the PI and PTFE films due to the smaller surface tension of PI as compared to that of PTFE. The polyimide film attracts ethanol, whereas the PTFE film repels it. Thus, flowing ethanol gas over the surface of the PI film will lead to a faster decrease in the output voltage.

When the ZnO nanowires are decorated with NiO nanoparticles and a PTFE layer is used, the output voltage significantly decreases to about 1.0 V, as shown in **Figure 4**a. This may be due to the increase in the resistance of the oxide, leading to a decrease in the triboelectric charge density on both surfaces.[36] The enhancement of the depletion layer due to the NiO nanoparticles decreased the electron concentration at the surface of the ZnO nanowires and increased the surface band bending, thereby, increasing the work function at the surface of the ZnO nanowires. This led to a decrease in the electron transfer to the PTFE layer, thereby decreasing the output performance of the TENG. The output voltage decreased by only about 0.14 V when exposed to the ethanol gas and the sensitivity was calculated to be about –0.15, which is twice smaller than that of the plain ZnO nanowires. It can also clearly be seen that the response time was slower (>10 min) in this TENG. This can be ascribed to the increase in the electron concentration because of electron transfer to the ZnO nanowires by the catalytic gas oxidation occurring on the nanowire surface. The increase in electron concentration decreased the surface band bending, indicating that the work function at the surface of ZnO decreased and the potential difference with the Fermi level of the dielectric layer increased. The modified surface energy diagram thus enhanced the electron transfer from ZnO to the dielectric materials, which in turn increased the triboelectric charge density at both surfaces, thereby, enhancing the output voltage of the TENG. Thus, the enhancement in the electrical output reduces the decrease in output voltage by the gas exposure. However, this mechanism is still under investigation.[37,38] The slow response time can also be explained by the slow increase in current of the NiO NPs-decorated ZnO nanowires by the chemical process at room temperature. When the PTFE was replaced by polyimide, the output voltage decreased to 0.2 V and the response time was faster (Figure 4b), which is consistent with the above results.

To further support the above results and our hypothesis, we calculated the electrostatic potential distributions between the ZnO nanowires and the PTFE layer, as shown in Figure S4 (Supporting Information). The material parameters of ZnO and PTFE, taken from COMSOL simulation software, were used for finite-element analysis. The dielectric constants of ZnO and PTFE were calculated to be 10.2 and 2.1 respectively. When the device was fully released, the electric potential of ZnO (U_{ZnO}) was assumed to be zero, and, therefore, the electric potential of PTFE (U_{PTFE}) could be expressed as $U_{PTFE} = \sigma d/\varepsilon_0$, where σ is the triboelectric

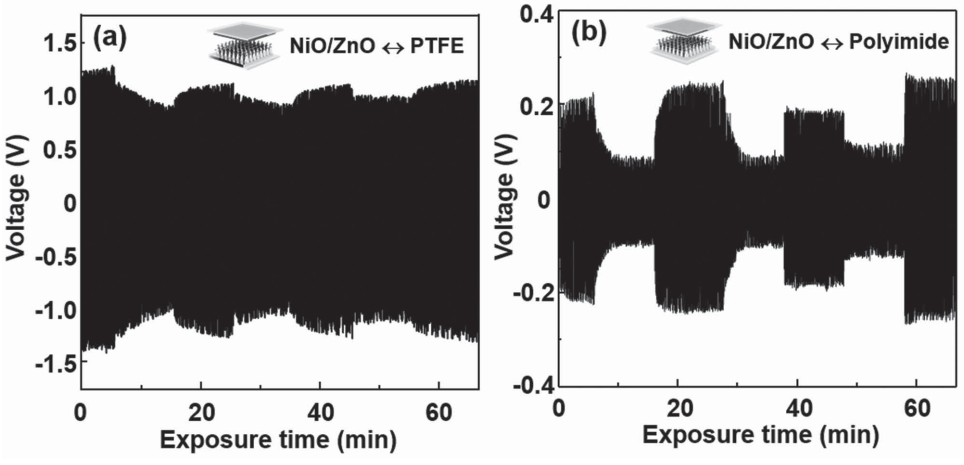

Figure 4. The output performance of the sensor elements comprising a) NiO NP-decorated ZnO-PFTE and b) NiO NP-decorated ZnO-PI under cycled compressive force of 50 N at an applied frequency of 4 Hz. The enlarged output voltages of each sensor element are also shown here.

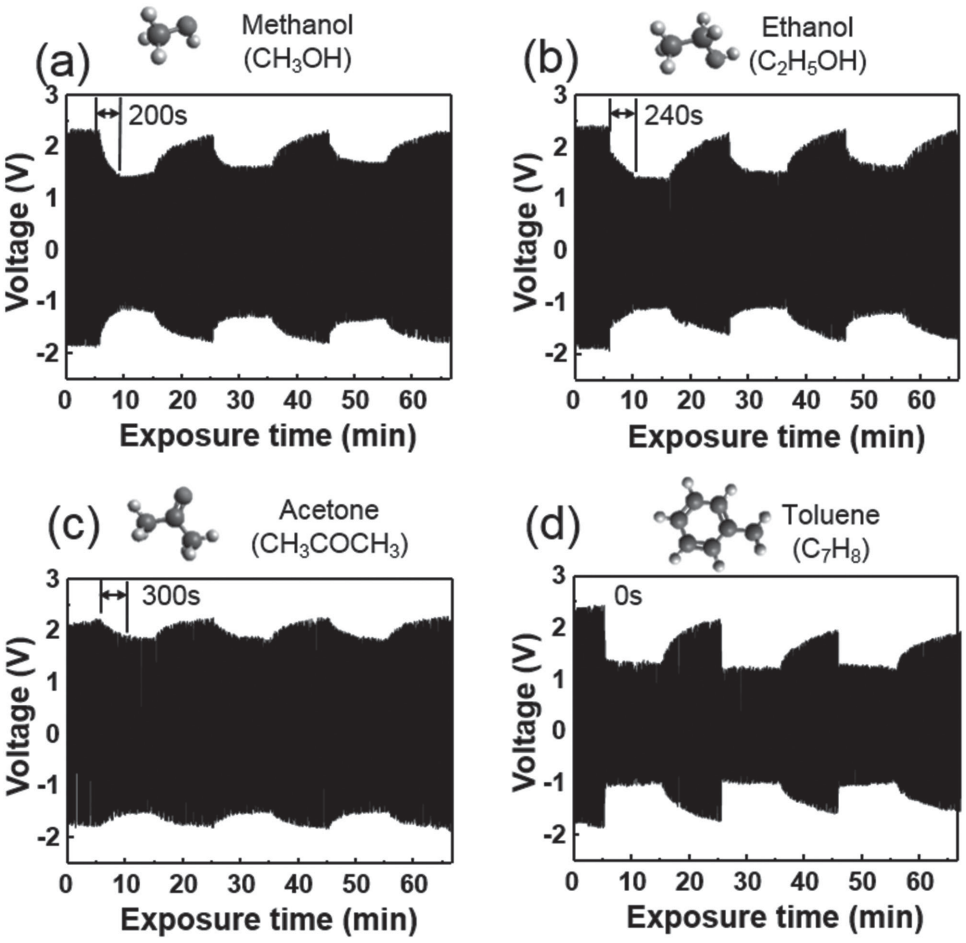

Figure 5. The output performances of the sensor with ZnO nanowires and a PTFE layer for the four different gases: a) methanol, b) ethanol, c) acetone, and d) toluene measured at room temperature.

charge density and ε_0 is the vacuum permittivity of free space (8.854×10^{-12} F m^{-1}). The gap distance (d) between the nanowires and the PTFE layer was approximately 1 mm. From the output voltages measured in ambient air (Figures 3a and 4a), the triboelectric charge density (Q_{air}) could be calculated as: $\sigma_{air} = \varepsilon_0 \cdot V/d$, and the values for the pristine ZnO and the NiO NP-decorated ZnO nanowires were 21.2 and 9.7 nC m^{-2}, respectively, under cycled compressive force.

In terms of the resistivity (ρ) of the nanowires, the triboelectric charge density (Q) can also be expressed as $Vt/\rho dA$,[39] where t is the measuring time and A is the contact area. Thus, the triboelectric charge density will increase with the conductivity ($\rho = 1/\sigma$) of the nanowires. Assuming that the change in electron concentration by the chemical reaction occurring on the nanowire surface is only one factor that affects the output power, the simulation shows that there is no change in electric potential when the ZnO nanowires are exposed to ethanol gas. However, for the NiO NPs-decorated ZnO nanowires, the triboelectric charge density increased up to 10.67 nC m^{-2}, which is a 10% increase, therefore, the electric potential increased, as shown in Figure S4 (Supporting Information). This simulation clearly confirms that the electron transfer by the heterogeneous catalytic reaction enhances the output performance of the TENG, by reducing the decrease in output voltage of the sensors.

Figure 5 shows the responses of a device consisting of ZnO nanowires and a PTFE layer toward the four VOC gases. Methanol gas decreased the output voltage from 2.4 V to 1.5 V after around 3 min of exposure to the gas at room temperature and the output voltage was returned to the original value after 10 min. For ethanol gas a similar response was found. For the acetone gas, the output voltage decreased to 1.8 V, indicating that the sensitivity significantly decreased, compared to that for the methanol and ethanol gases. It should also be noted that the response time was slower. Of the four gases, only acetone gas significantly increased the conductivity of the nanowires, indicating that the behavior toward the gas can be ascribed to the electron transfer from the gas molecules to the ZnO nanowires. The simulation in Figure S5 (Supporting Information) also supports that the output voltage increased when the TENG was exposed to only acetone gas. Note that the response of the device toward toluene gas is very fast. The output voltage dramatically decreased within 6 s after toluene exposure. This may be due to the non-polar characteristics of the gas, which increases the degree of wettability of the surface of the gas. In general, the greater the polar proportion (e.g O–H, C=O) in a

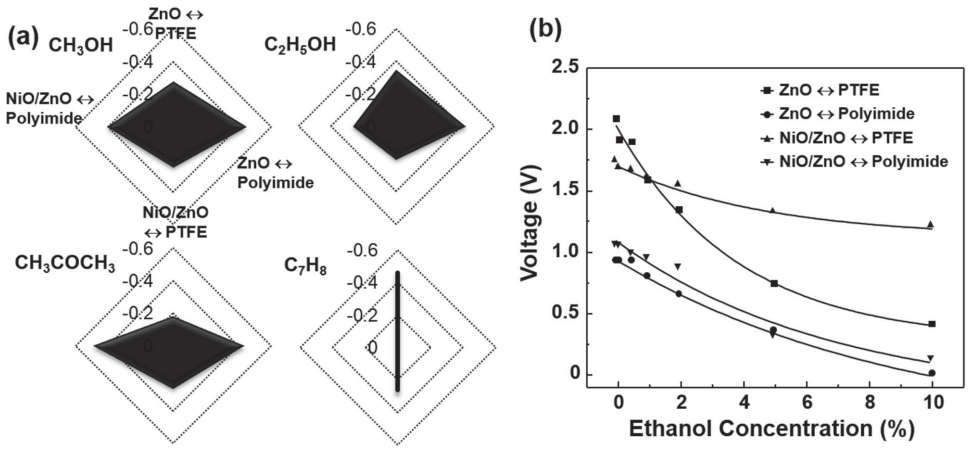

Figure 6. Radial plots of methanol, ethanol, acetone, and toluene gas responses over each sensor showing that they are prominently different. b) The output voltage of each sensor element with increasing concentration of ethanol gas from 0.1% to 10%.

molecule, the stronger the attractive forces between a gas molecule and a surface, causing a greater tendency to form discrete droplets on the surface rather than wet it evenly.[40,41] Thus, for the non-polar toluene (0.36 D), the molecules tend to spread on the surface quickly, thereby decreasing the voltage quickly.[42]

As can be seen from **Figure 6**a, the radial plots of methanol, ethanol, acetone, and toluene gas responses over each sensor are prominently different for the four different systems. This result indicates that although the sensor responses are also influenced by other parameters, the sensor design based on triboelectrification and heterogeneous catalytic reaction can be a promising platform to enhance the degree of selectivity. In the present case, the sensitivities were derived from the steady-state output voltage differentials of each of the sensor elements when exposed to one of the four gases, as shown in Figure S1 (Supporting Information). However, it seems that the radial plots of the methanol and ethanol gases are similar, which may be acribed to the properties of both gases, such as surface tension and molecular structure, being so similar. This may be solved by increasing the number of sensor elements, such as by using various catalytic materials (Pd, Pt, etc.) or dielectric layers (PMMA, etc.). By also taking into account the response time, the discrimination ability becomes better. Figure 6b shows that the output voltages of the TENGs decreased with increasing ethanol concentration from 0.1% to 10%, with a logarithmical scale. This implies that the electrical performance of the TENGs is dominated by electron transfer as the concentration increases. This approach provides a detection limit of 0.1% at room temperature.

3. Conclusions

A self-powered, room-temperature electronic nose strategy with highly selective gas detection was described, which is based on triboelectrification by the physical contact between the ZnO nanowires and the dielectric layers, and the heterogeneous catalytic reaction occurring on the nanowires and on the NiO nanoparticles. The electronic nose is a two-dimensional microarray where the individual sections orthogonally vary in their properties on account of two response-modifying strategies. Along one axis a NiO nanoparticle functionality was applied to the ZnO nanowires. The NiO functionality was found to be more reactive for all VOC gases, whereas only acetone gas was reactive on the surface of the ZnO nanowires due to its small dissociation energy. The electron transfer to the nanowires by the catalytic oxidation increased the triboelectric charge density at both surfaces, thereby increasing the output voltage of the devices. This was clearly supported by COMSOL simulations. The slow response time also supported the contribution of the catalytic oxidation to the output power. Two dielectric layers (PTFE and polyimide) with different surface tensions were then placed along the orthogonal axis. When the surfaces are exposed to the VOC gases, the output voltage decreased because the molecular species on both surfaces reduced the triboelectrically charged area. The sensor comprising a polyimide layer showed a faster response than the one including a PTFE layer, because of the higher surface energy of PI compared to that of PTFE. The response time was also strongly dependent on the portion of polar groups in the molecule.

The sensors were then tested for their ability to distinguish between four VOC gases (methanol, ethanol, acetone, and toluene), in which discrimination between the gases could be achieved using the electronic nose approach through an analysis of the responses. This approach also provided a detection limit of 0.1% at room temperature. Although it is still difficult to distinguish between the methanol and ethanol gases, it is believed that a strong discriminating power can be accomplished by tuning the sensitivities and the response times of the sensor elements. The self-powered sensors may be applicable in many places with limited accessibility to monitor gases and chemicals over long periods of time or in portable applications, such as electronic skins or textiles.

4. Experimental Section

ZnO Nanowires Synthesis and Characterization: ZnO nanowires were synthesized on a 100-nm thick ZnO film on a SiO_2 wafer by RF sputtering. The ZnO film was patterned and separated into 4 sections. There was no electrical connection between them. Before the growth,

the substrate was loaded into a UV–ozone treatment chamber to enhance the growth of ZnO nanostructures. The substrates were then put facing down on the growth solution (1:1 ratio of zinc nitrate and hexamethylenetetramine (HMTA) 2 mM) and were kept in an oven at 90 °C for 10 h. After the growth, SEM images clearly showed that the nanowires covered the surface of the patterned substrates uniformly and compactly. 5-nm thick (mass thickness) Ni films were deposited using an electron-beam evaporator at a base pressure of 3.0×10^{-6} Torr through a shadow mask to functionalize the surface of the nanowires. The metal films are aggregated into well-separated NiO nanoparticles after annealing at 600 °C for 30 min.

Electronic Nose Fabrication: An Al thin film, acting as the top electrode, was prepared and adhered onto either a polyimide or PTFE film (1 cm × 1 cm) with a thickness of 0.03 mm, producing 2 × 2 arrays. When the fabrication process was complete each 2 × 2 array functioned as one "sensor element"; and each sensor element corresponded to a unique combination of dielectric materials and NiO nanoparticle decoration.

The devices were placed in a reaction chamber and exposed to pulses of one of four VOC gases (1% methanol, ethanol, acetone, or toluene) under room temperature and air-conditioned atmosphere with a flow rate of 1000 sccm. The device was connected with the electrical measurement systems, which independently monitored the change in output voltage under dynamic conditions when the device was exposed to the gases. The output voltage of the device was recorded using a digital sourcemeter (Keithley model 2400) under a cycled compressive force of 50 N at the frequency of 4 Hz. The sensor response was defined as the sensitivity ($S = 100 \times (V_g - V_a)/V_a$), where V_g and V_a are the output voltages measured in the presence of VOC gases and air, respectively.

Supporting Information

Supporting Information is available from the Wiley Online Library or from the author.

Acknowledgements

This research was supported by Basic Science Research Program through the National Research Foundation of Korea (NRF) funded by the Ministry of Science, ICT and Future Planning (2012R1A1A1044091), by the KIST-UNIST partnership program (2V03870/2V03880) or equivalently by the 2014 Research Fund (1.140019.01) of UNIST (Ulsan National Institute of Science and Technology), and by Technology Innovation Program (10054548, Development of Suspended Heterogeneous Nanostructure-based Hazardous Gas Microsensor System) funded by the Ministry of Trade, industry & Energy (MI, Korea).

Received: August 14, 2015
Revised: September 11, 2015
Published online: October 19, 2015

[1] V. V. Sysoev, J. Goschnick, T. Schneider, E. Strelcov, A. Kolmakov, *Nano Lett.* **2007**, *7*, 3182.
[2] J. Homola, *Chem. Rev.* **2008**, *108*, 462.
[3] Z. Hu, B. J. Deibert, J. Li, *Chem. Soc. Rev.* **2014**, *43*, 5815.
[4] J. R. Askim, M. Mahmoudi, K. S. Suslic, *Chem. Soc. Rev.* **2013**, *42*, 8649.
[5] J. M. Baik, M. Zielke, M. H. Kim, K. L. Turner, A. M. Wodtke, M. Moskovits, *ACS Nano* **2010**, *4*, 3117.
[6] W. J. Park, K. J. Choi, M. H. Kim, B. H. Koo, J. L. Lee, J. M. Baik, *ACS Appl. Mater. Interfaces* **2013**, *5*, 6802.
[7] C. Yu, Q. Hao, S. Saha, L. Shi, X. Kong, Z. L. Wang, *Appl. Phys. Lett.* **2005**, *86*, 063101.
[8] J. D. Prades, R. J. Diaz, F. H. Ramirez, S. Barth, A. Cirera, A. R. Rodriguez, S. Mathur, J. R. Morante, *Appl. Phys. Lett.* **2008**, *93*, 123110.
[9] H. Zhang, Y. Yang, Y. Su, J. Chen, C. Hu, Z. Wu, Y. Liu, C. P. Wong, Y. Bando, Z. L. Wang, *Nano Energy* **2013**, *2*, 693.
[10] Z. Li, J. Chen, J. Yang, Y. Su, X. Fan, Y. Wu, C. Yub, Z. L. Wang, *Energy Environ. Sci.* **2015**, *8*, 887.
[11] Z. H. Lin, G. Zhu, Y. S. Zhou, Y. Yang, P. Bai, J. Chen, Z. L. Wang, *Angew. Chem. Int. Ed.* **2013**, *52*, 5065.
[12] Y. Lin, P. Deng, Y. Nie, Y. Hu, L. Xing, Y Zhang, X. Xue, *Nanoscale* **2014**, *6*, 4604.
[13] X. Xue, Y. Nie, B. He, L. Xing, Y. Zhang, Z. L. Wang, *Nanotechnology* **2013**, *24*, 225501.
[14] Z. Qu, Y. Fu, B. Yu, P. Deng, L. Xing, X. Xue, *Sens. Actuators B* **2016**, *222*, 78.
[15] Z. H. Lin, G. Cheng, W. Wu, K. C. Pradel, Z. L. Wang, *ACS Nano* **2014**, *8*, 6440.
[16] N. J. Kybert, M. B. Lerner, J. S. Yodh, G. Preti, A. T. C. Johnson, *ACS Nano* **2013**, *7*, 2800.
[17] Z. Dai, L. Xu, G. Duan, T. Li, H. Zhang, Y. Li, Y. Wang, Y. Wang, W. Cai, *Sci. Rep.* **2013**, *3*, 1669.
[18] C. Kaewsaneha, P. Tangboriboonrat, D. Polpanich, M. Eissa, A. Elaissari, *ACS Appl. Mater. Interfaces* **2013**, *5*, 1857.
[19] E. Barea, C. Montoro, J. A. R. Navarro, *Chem. Soc. Rev.* **2014**, *43*, 5419.
[20] C. S. Prajapati, P. P. Sahay, *Sens. Actuators B* **2011**, *160*, 1043.
[21] J. Xu, X. Jia, X. Lou, G. Xi, J. Han, Q. Gao, *Sens. Actuators B* **2007**, *120*, 694.
[22] J. Xu, J. Han, Y. Zhang, Y. Sun, B. Xie, *Sens. Actuators B* **2008**, *132*, 334.
[23] G. K. Mani, J. B. B. Rayappan, *Sens. Actuators B* **2014**, *198*, 125.
[24] Y. Liu, G. Li, R. Mi, C. Deng, P. Gao, *Sens. Actuators B* **2014**, *191*, 537.
[25] C. W. Na, H. S. Woo, J. H. Lee, *RSC Adv.* **2012**, *2*, 414.
[26] Z. Lou, L. Wang, T. Fei, T. Zhang, *New J. Chem.* **2012**, *36*, 1003.
[27] D. Ju, H. Xu, Z. Qiu, J. Guo, J. Zhang, B. Cao, *Sens. Actuators B* **2014**, *200*, 288.
[28] G. K. Mani, J. B. B. Rayappan, *Sens. Actuators B* **2013**, *183*, 459.
[29] M. R. Yu, G. Suyambrakasam, R. J. Wu, M. Chavali, *Mater. Res. Bull.* **2012**, *47*, 1713.
[30] G. Zhu, Z.-H. Lin, Q. Jing, P. Bai, C. Pan, Y. Yang, Y. Zhou, Z. L. Wang, *Nano Lett.* **2013**, *13*, 847.
[31] S. Wang, L. Lin, Z. L. Wang, *Nano Lett.* **2012**, *12*, 6339.
[32] P. Bai, G. Zhu, Y. Liu, J. Chen, Q. Jing, W. Yang, J. Ma, G. Zhang, Z. L. Wang, *ACS Nano* **2013**, *7*, 6361.
[33] Y. H. Ko, G. Nagaraju, S. H. Lee, J. S. Yu, *ACS Appl. Mater. Interfaces* **2014**, *6*, 6631.
[34] S. Niu, Y. Hu, X. Wen,Y. Zhou, F. Zhang, L. Lin, S. Wang, Z. L. Wang, *Adv. Mater.* **2013**, *25*, 3701.
[35] R. Yu, C. Pana, Z. L. Wang, *Energy Environ. Sci.* **2013**, *6*, 494.
[36] Z. H. Lin, G. Cheng, Y. Yang, Y. S. Zhou, S. Lee, Z. L. Wang, *Adv. Funct. Mater.* **2014**, *24*, 2810.
[37] L. S. McCarty, G. M. Whitesides, *Angew. Chem. Int. Ed.* **2008**, *47*, 2188.
[38] V. Nguyen, R. Yang, *Nano Energy* **2013**, *2*, 604.
[39] Y.-P. Chang, Y.-C. Chiou, R.-T. Lee, *Wear* **2004**, *257*, 347.
[40] G. Wang, L. Zhang, J. Zhang, *Chem. Soc. Rev.* **2012**, *41*, 797.
[41] X. J. Feng, L. Jiang, *Adv. Mater.* **2006**, *18*, 3063.
[42] B. P. Binks, A. Rocher, *Phys. Chem. Chem. Phys.* **2010**, *12*, 9169.